Materials and Design 89 (2016) 1123–1129

Contents lists available at ScienceDirect

Materials and Design

journal homepage: www.elsevier.com/locate/jmad

Structure and residual stress evolution of Ti/Al, Cr/Al or W/Al co-doped amorphous carbon nanocomposite films: Insights from ab initio calculations

Xiaowei Li *, Lili Sun, Peng Guo, Peiling Ke, Aiying Wang *

Key Laboratory of Marine Materials and Related Technologies, Key Laboratory of Marine Materials and Protective Technologies of Zhejiang Province, Ningbo Institute of Materials Technology and Engineering, Chinese Academy of Sciences, Ningbo 315201, P.R. China

ARTICLE INFO

Article history:
Received 2 August 2015
Received in revised form 6 October 2015
Accepted 19 October 2015
Available online 20 October 2015

Keywords:
Stress
Bond structure
Co-doping
Amorphous carbon
Ab initio calculation

ABSTRACT

Here, we selected Ti, Cr, and W as the representative metal elements to composite with Al atom in order to generate co-doped amorphous carbon (a-C) films using ab initio calculations. Results show that compared with the pure and mono-doped cases, the Ti/Al, Cr/Al, or W/Al co-doped a-C films exhibit a general tendency of stress reduction. Particularly, it is noted that with the co-doping of Ti (1.56 at.%)/Al (1.56 at.%), Cr (1.56 at.%)/Al (4.69 at.%), or W (1.56 at.%)/Al (1.56 at.%), the residual stress is reduced by 83%, 78.9%, and 90.6%, respectively, without deteriorating the mechanical properties. Structural analysis reveals that the co-doping of Ti/Al, Cr/Al, or W/Al brings the critical and significant relaxation of distorted C–C bond lengths, as well as the formation of a weak covalent interaction for Ti–C, Cr–C, and W–C bonds and the ionic interaction for Al–C bonds, which account for the giant residual stress reduction. Consequently, by the synergistic effect of small amounts of soft ductile weak-carbide-forming metals and hard-carbide ones, it provides the theoretical guidance and desirable strategy to design and fabricate the a-C films with low residual stress and other novel performance/functions.

1. Introduction

Amorphous carbon (a-C) films have emerged as the key ingredients for the developments of many protective materials and advanced devices [1–3]. In particular, nanostructuring a-C films with metal dopants renews them more potential applications ranging from electronic and biological to automotive tribological industry, due to the enhanced physicochemical properties and multi-functionalities [4–8]. Despite the versatile features of metal dopants and classifications of a-C films, it is generally observed that metal doped a-C films consist of the nanocrystallites of pure metal or metal carbides embedded in the amorphous carbon matrix [9–11]. In comparison to pure a-C films, the most known benefit of metal dopants is the considerable reduction of residual compressive stress, which is attributed to the promoted graphitization of C-sp^2 bonds [12], substitution of strong C–C bonds by weak Me–C bonds [13], or pivot site of metal nanocrystallites for structure relaxation [14]. So far, however, since these stress reductions induced by single metal dopant are always at a sacrifice of mechanical or tribological properties of carbon films in most previous works [12–16], there is a critical pre-requisite to overcome these barriers by taking full advantages of multiple nanostructures co-existing in carbon films.

Recently, multiple metal elements co-doping has been taken into account recently to overcome these barriers and explore new functions. Jansson et al. [17] put forward a general concept to design the self-adaptive low friction nanocomposite coatings, where the Ti–Al–C was chosen for the model system. They found that alloying Al provided the driving force for the formation of amorphous carbon bonds, which promoted the graphitization of film during friction test and as a consequence, the friction coefficient was significantly reduced about 85% in $(Ti_{0.5}Al_{0.5})C_{1.2}$ coating compared to that of $TiC_{1.5}$. Similar results were also reported in Ti/Al co-doped amorphous hydrogenated carbon (a-C:H) films by Liu et al. [18,19], which exhibited the low residual stress, high toughness, low friction coefficient and wear rate. Moreover, when Ti was replaced by Si, due to the formed self-assembled dual metallic nanostructures combined with fullerene-like clusters in carbon matrix, a near-frictionless and extremely-elastic behavior but low hardness was obtained in Si/Al co-doped a-C:H film [20]. However, though the aforementioned results inspire that co-doping two metal elements in a-C films provides the desirable combination of tribological and mechanical properties for widely potential applications, the dependence of mechanical properties on structure of multiple metal co-existing a-C films from the viewpoint of atomic and electronic scale has not yet been studied, and it is also indispensable for clarifying the stress reduction mechanism and tailoring the excellent overall performance of a-C films.

In the present work, we focused on the residual stress and structure evolution of metal co-doped a-C films using ab initio calculations based

* Corresponding authors.
E-mail addresses: lixw@nimte.ac.cn (X. Li), aywang@nimte.ac.cn (A. Wang).

http://dx.doi.org/10.1016/j.matdes.2015.10.106
0264-1275/

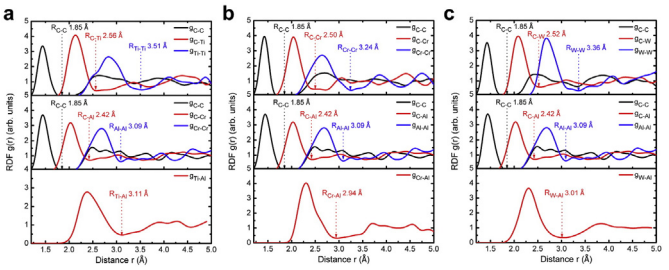

Fig. 1. RDF of (a) Ti/Al, (b) Cr/Al, and (c) W/Al mono- and co-doped a-C films with high Ti, Cr, W, and/or Al concentrations of 39 at.%, where the inset values are the R_{cut} values for the C–C, C–Me, and Me–Me bonds.

on density functional theory (DFT). Hard-carbide-forming metals (Ti, Cr, or W) and soft ductile weak-carbide-forming metals (Al) were selected as the representative doped metal elements to composite the co-doped systems. The residual stress and bulk modulus were calculated, and the bond structure including bond angles and bond lengths and bonding feature were examined to elucidate the stress reduction mechanism induced by co-dopants. We observed that co-doping Ti/Al, Cr/Al, or W/Al into a-C films into carbon matrix could exhibit an extremely low residual compressive stress due to the relaxation of highly distorted bond structures and the formation of weak bond characteristics in carbon matrix in comparison with that of Ti, Cr, W, or Al mono-doped and pure a-C films. If one notes the optimized designing with the selected co-doped metal characteristics, our results could not only account for the physical and chemical properties in experiment, but also present a new straightforward strategy to tailor the a-C films with low residual stress and other novel performance/functions.

2. Computational details

Compared with classical molecular dynamics (MD) methods which require predetermined empirical potential parameters for specified compositions, the superiority of the parameter-free ab initio simulation method is obvious. All the spin-polarized calculations were carried out using the Vienna ab initio simulation package based on DFT [21,22] with a cutoff energy of 500 eV and a generalized gradient approximation with the Perdew–Burke–Ernzerhof parameterization [23]. In this work, the initial configuration contained 64 atoms in a simple cubic supercell with constant volume and under periodic boundary conditions throughout the simulation that has been proved to be suitable and accurate to reveal the characteristics of amorphous carbon systems and also save the required computation time [24–26]. To obtain Ti/Al, Cr/Al, or W/Al co-doped a-C systems, a two-step process composed of melt-quenching by ab initio MD (AIMD) simulation and geometric optimization by static calculations was used, which has been demonstrated to give a good description of a-C materials and revealed the intrinsic relation between the structure and properties [25,27–29].

During the AIMD simulation, the system was first equilibrated at 8000 K for 1 ps to become completely liquid and eliminate its correlation to the initial configuration using *NVT* ensemble with a Nose thermostat for temperature-control and a time step of 1 fs; then, the samples were quenched from 8000 to 1 K at cooling rate of 1.6×10^{16} K/s. For the subsequent geometric optimization of amorphous structure, a full relaxation of the atomic positions based on conjugated gradient method [30] was repeated until the Hellmann–Feynman force on each atom was below 0.01 eV/Å, and the self-consistent loop was created using an energy convergence criterion of 10^{-5} eV; a gamma point only was used to sample the Brillouin zone. To check the *k*-point convergence on amorphous structure, a fully converged calculation with a grid of $4 \times 4 \times 4$ points (64 *k* points) was performed. When the gamma point only was used, compared to a fully converged calculation with 64 *k* points, the absolute error of average binding energy of per atom was found to be accurate to better than 0.004 eV.

Since we focused on the small amount of co-doped metal concentration without invoking severe changes in carbon matrix, the total concentrations for two metals in Ti/Al, Cr/Al, or W/Al co-doped systems were selected ranging from 3.12 to 7.81 at.% with different ratios, corresponding to 2, 3, 4 and 5 atoms in 64-atom systems, respectively. In order to provide more representative models of the real metal doped system than the direct substitution of carbon by metal atoms in pre-generated pure carbon networks, Ti, Cr, or W with Al atoms were introduced by substituting carbon atoms in the liquid carbon state with an external equilibrium at 8000 K for 0.5 ps [25,29]. Pure and mono-doped a-C films were also involved for comparison with the co-doped ones.

3. Results and discussion

Before characterizing the structure of Ti/Al, Cr/Al, and W/Al co-doped a-C films, the RDF, g(r), in the systems with high metal concentration was analyzed firstly to define the Ti, Cr, W, Al, and C atoms being bonded or non-bonded with each other, as shown in Fig. 1. The distance to the first minimum in RDF (inset values of Fig. 1) was set as the cutoff distance R_{cut} for the C–C, C–Me, and Me–Me bonds [24,31]. Then, the RDF, final morphologies, residual compressive stress, bulk modulus, both the bond angle and bond length distributions and electronic structure in various a-C systems were evaluated.

Fig. 2 shows the final structures of Ti/Al co-doped a-C films by using the cutoff distance of Fig. 1 to determine the nearest neighbor atoms. Pure and Ti/Al mono-doped cases are also considered. We find that all the films are amorphous, which will be described later by RDF. Fig. 3

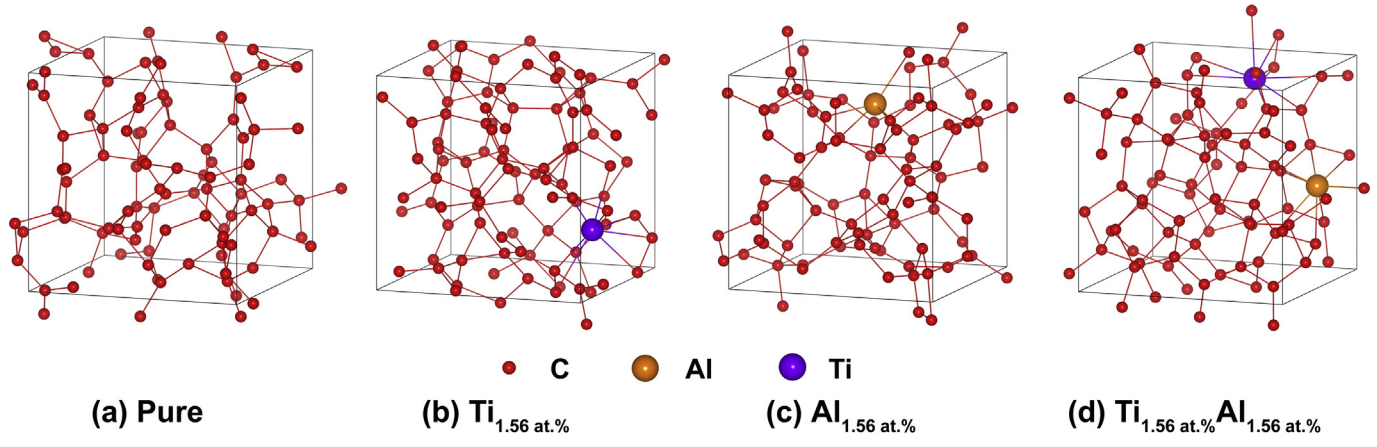

Fig. 2. Atomic structures of pure a-C, Ti/Al mono- and co-doped a-C films, in which the subscript is the concentration of each doped metal atoms.

gives the tetra-coordinated C content for each case. For pure a-C film, the structure is dense, and the tetra-coordinated C content is 56.2% (Fig. 3), which is consistent with previous work [28]. However, in Ti doped a-C films, the tetra-coordinated C hybridized structure with the addition of Ti increases at first, because the doped Ti atoms could easily bond with the three-coordinated C atoms with low bonding energy, which agrees well with the experimental results [32]. With further increasing Ti content to 7.81 at.%, the formation of many highly distorted five-coordinated C atoms with the content of 14.06% causes the decrease of tetra-coordinated C content, suggesting the high residual compressive stress [24]. In Al doped a-C films (Fig. 3), the similar behavior of hybridized structure with Al content is also observed. However, co-doping Ti/Al into carbon matrix seems to modify the structure seriously, as illustrated in Figs. 2d and 3, which will induce the significant change of properties; after co-doping Ti 1.56 at.% and Al 1.56 at.% into the a-C film simultaneously, the tetra-coordinated C content of 73.44% is obtained. Besides, noted that for the co-doped films with constant Ti content, the tetra-coordinated C content as a function of Al content decreases gradually following the increase of three-coordinated C content and five-coordinated hybridized structures.

Fig. 4 shows the RDF spectra of pure, Ti/Al mono- and co-doped a-C films. First, it reveals that for each case the film shows the typical amorphous character, that is long-range disorder and short-range order. For pure a-C film, the 1st nearest neighbor peak is located at 1.50 Å, which is in agreement with the previous experimental [33,34] and theoretical results [25,28,35], suggesting that the simulated results reflect the nature of real system. As known that the 1st peak is related with the atomic bond lengths, and the 2nd peak correlates with both the bond angles and bond lengths. The position of 1st peak in pure a-C film is much smaller than that of diamond, which implies the high residual compressive stress [36]. After the addition of Ti and/or Al into the films, the positions of the 1st and 2nd nearest neighbor peaks in RDF are deviated from that of pure a-C film. By mono- and co-doping Ti 1.56 at.% and Al 1.56 at.% into a-C film shown in Fig. 4, the positions of 1st nearest-neighbor peak shift to 1.51, 1.51 and 1.52 Å, respectively, demonstrating the evolution of atomic bond structure and properties.

The biaxial stress, σ, and bulk modulus, B, are computed by the equations

$$P = \frac{P_{xx} + P_{yy} + P_{zz}}{3} \quad (1)$$

$$B = -V\frac{dP}{dV} \quad (2)$$

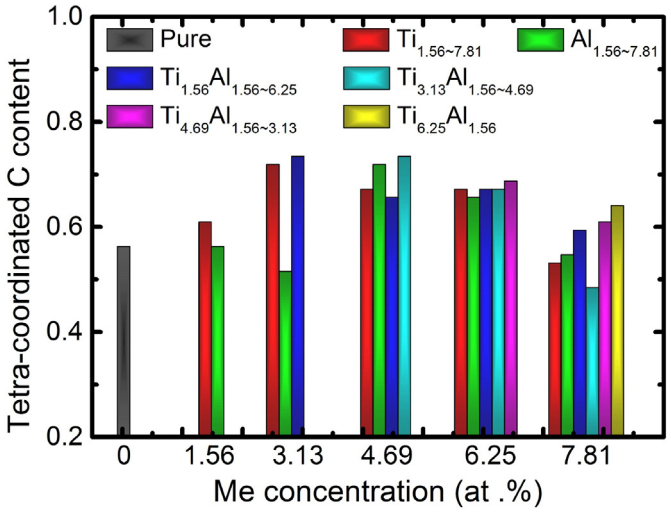

Fig. 3. Tetra-coordinated C content of pure a-C, Ti/Al mono- and co-doped a-C films, in which the subscript is the concentration of each doped metal atoms.

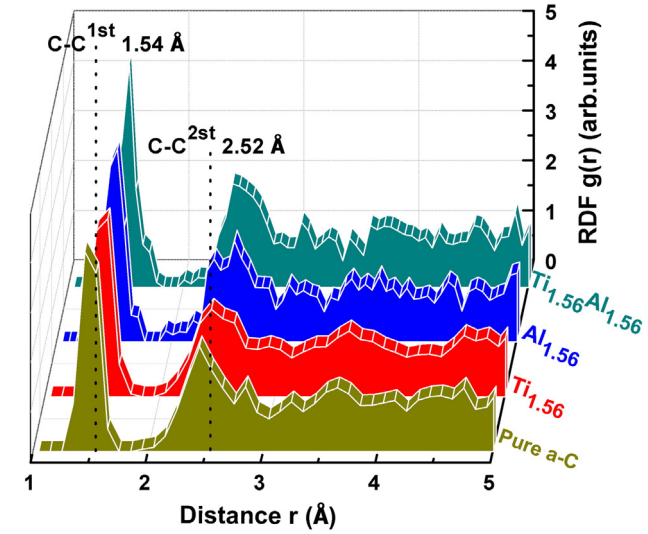

Fig. 4. RDF spectra of pure, Ti/Al mono- and co-doped a-C films. The vertical dotted lines represent the 1st and 2nd nearest peak positions of crystalline diamond; the subscript is the concentration of each doped metal atoms.

$$\sigma = \frac{3}{2}P \quad (3)$$

where P is the hydrostatic pressure, P_{xx}, P_{yy} and P_{zz} are the diagonal components of the stress tensor, V is the system volume, B is the bulk modulus; the pressure, P, is converted to the biaxial stress, σ, by multiplying the pressure by a factor of 1.5, according to the method of McKenzie (Eq. (3)) [37,38], which expresses the hydrostatic pressure as the average of the diagonal components of the stress tensor. Fig. 5 shows the residual compressive stress and bulk modulus of Ti/Al co-doped a-C films as a function of Ti/Al concentrations. Pure and Ti/Al mono-doped cases are also evaluated. Our previous study [24] presents that in case of the pure a-C film, a high residual compressive stress about

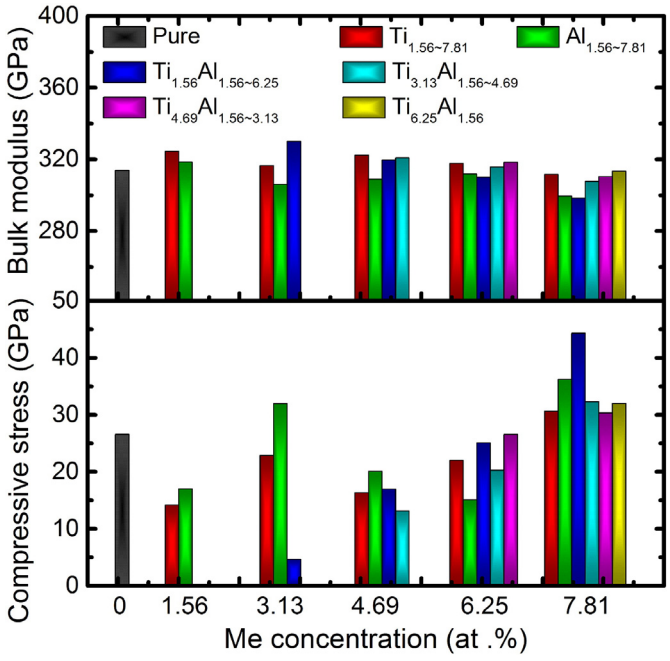

Fig. 5. Compressive stress and bulk modulus of pure, Ti/Al mono- and co-doped a-C films as a function of Ti/Al concentrations. The subscript is the concentration of each doped metal atoms.

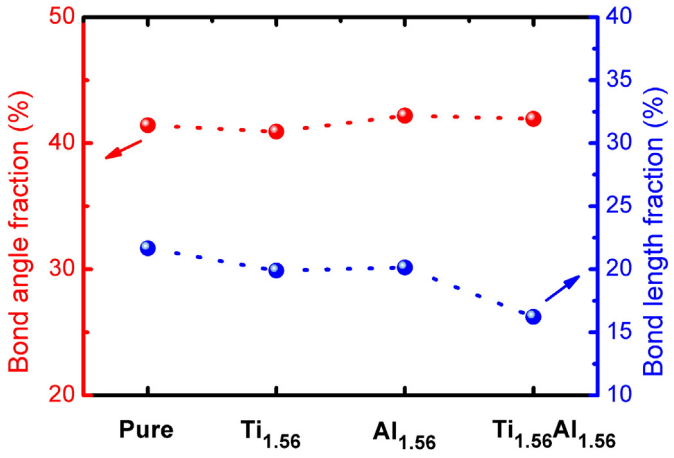

Fig. 6. Fractions of distorted bond angles (<109.5°) and bond lengths (<1.42 Å) in pure, Ti/Al mono-doped and co-doped a-C films. The subscript is the concentration of each doped metal atoms in the film.

26.6 GPa is estimated; for Ti doped a-C films, the compressive stress with Ti concentrations decreases firstly and then increases, which has been proved in previous experimental study [32]. When the Ti concentration is 1.56 at.%, the minimal residual compressive stress of about 14.2 GPa is obtained [24]. In addition, the bulk modulus changes slightly, which is in accordance with the change of tetra-coordinated C content shown in Fig. 3. In general, the mechanical properties of a-C films mainly depend on the tetra-coordinated C interlink matrix. This can account for the behavior of bulk modulus with Ti concentrations and also proves that Ti as a hard-carbide formatting metal has little effect on mechanical properties [32]. For Al doped a-C films, the evolution of residual stress with Al concentrations is similar to that in Ti doped cases, and a lower compressive stress of about 17.0 GPa is generated in the film with Al 1.56 at.%; moreover, noted that the doped soft ductile weak-carbide forming metals, Al, gives rise to the obvious decrease of bulk modulus from 318.4 to 299.5 GPa [12].

However, after introducing Ti and Al into a-C films simultaneously, the drastic evolution of residual stress is presented in Fig. 5 and the bulk modulus also shows the similar behavior to that of the tetra-coordinated C content (Fig. 3). As the concentrations of Ti and Al are 1.56 and 1.56 at.%, respectively, the film exhibits the lowest residual

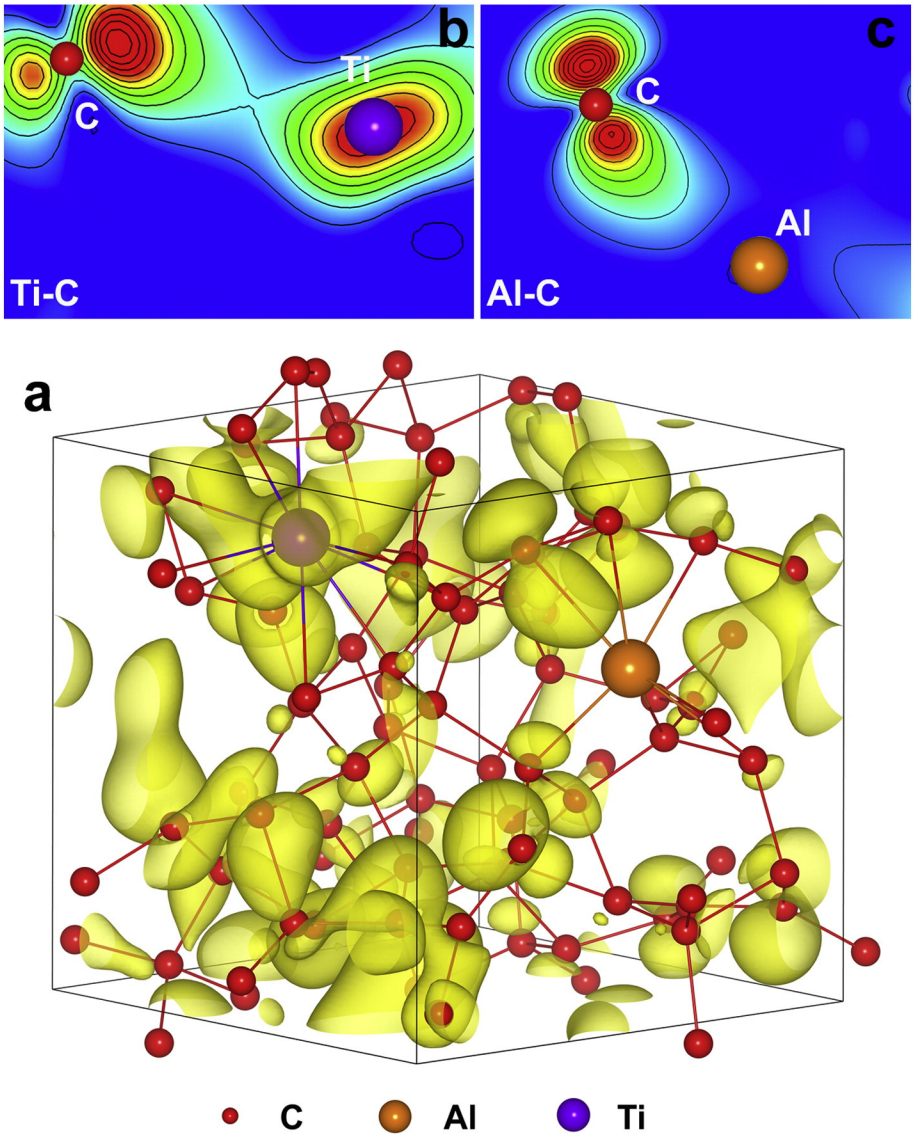

Fig. 7. (a) Charge density of HOMO for the Ti/Al co-doped a-C system with Ti 1.56 at.% and Al 1.56 at.%. (b) and (c) are the contour plots of charge density of HOMO passing through Ti–C or Al–C bond, respectively.

stress of about 4.6 GPa. In respect to pure a-C film, co-doping Ti and Al could reduce the residual stress by 83%, while in Ti/Al mono-doped cases the stress only drops by 47% or 36%, respectively. This is well consistent with previous work [19], in which the residual stress of Ti/Al co-doped a-C film decreased about 50% comparing to that of Ti doped a-C film. Most importantly, the co-doping of Ti (1.56 at.%) and Al (1.56 at.%) brings the bulk modulus slightly increased to 329.9 from 324.4 (only Ti) and 318.4 GPa (only Al). This suggests that compared with the Ti/Al mono-doping, co-doping a small amount of Ti/Al into a-C films could not only reduce the compressive stress drastically, but also retain the excellent mechanical properties which are usually deteriorated by doping single metal atoms [12–14].

In order to elucidate the properties in terms of the doped metal concentrations and provide further insight to the stress reduction mechanism, more direct evidences for the atomic bond structure including both the bond angle and length distributions of Ti/Al co-doped a-C films are analyzed firstly. Previous study has revealed that the high residual compressive stress of a-C films is mainly originated from the distortion of both the bond angles and bond lengths of carbon network, which are less than 109.5° and 1.42 Å, respectively [24,36]. So the C–C–C bond angles and C–C bond length distributions in pure, Ti/Al mono- and co-doped a-C films are integrated to gain the fractions of distorted bond angles (<109.5°) and bond lengths (<1.42 Å), as shown in Fig. 6. In pure a-C film, the fraction of distorted bond angles is 41.4% and that of distorted bond lengths is 21.7% [24]. By mono-doping Ti 1.56 at.% into a-C film, the fractions of distorted bond angles and bond lengths are decreased to 40.9% and 19.9% separately, leading to the decrease of residual compressive stress (Fig. 5) [24]; but in Al mono-doped film with Al 1.56 at.%, doping Al into a-C film causes the opposite changes in the fractions of distorted bond angles and bond lengths which are 42.1% and 20.1%, respectively. As a consequence, this leads to the mediate change in the residual stress (Fig. 5). Nevertheless, after co-doping Ti (1.56 at.%) and Al (1.56 at.%) into films, the synergistic effect of Ti and Al atoms on the structure brings the fraction of distorted bond lengths to be significantly decreased to 16.2%, while the fraction of distorted bond angles slightly increases to 41.9%. This contribution agrees well with the calculation results (Fig. 5) and experiments study where a drastic reduction of residual stress is visible [19].

In addition, the evolution of electronic structure such as the bonding characteristics caused by Ti/Al co-doping is also of great importance for optimizing the design strategies and providing the further insight for the residual stress reduction mechanism. The spin resolved density of states shows that the obvious hybridization occurs between Ti-3*d*, Al-3*s* or Al-3*p* and C-2*p* atomic orbitals, and the highest occupied molecular orbital (HOMO) mainly consists of Ti-3*d*, Al-3*p* and C-2*p* atomic orbitals. The charge density distribution of HOMO is given in Fig. 7. It illustrates that the Ti and C atoms are connected by the charge distribution (Fig. 7b). This is the typical character of covalent bond, but the charge accumulation between Ti and C atoms is much smaller than C–C covalent bond [36], suggesting the weak bond strength. Especially, the charge between Al and C atoms in the HOMO is concentrated around the more electronegative atom, C (Fig. 7c). This indicates that the bond characteristic between Al and C atoms is ionic. Since the HOMO characteristics also contributes to the system rigidity except the tetra-coordinated C content, the Ti and Al atoms could form the weak covalent for Ti–C and ionic bond for Al–C separately in Ti/Al co-doped a-C systems and thus play the role of a pivotal site to reduce the bond strength and directionality drastically, where the distortion

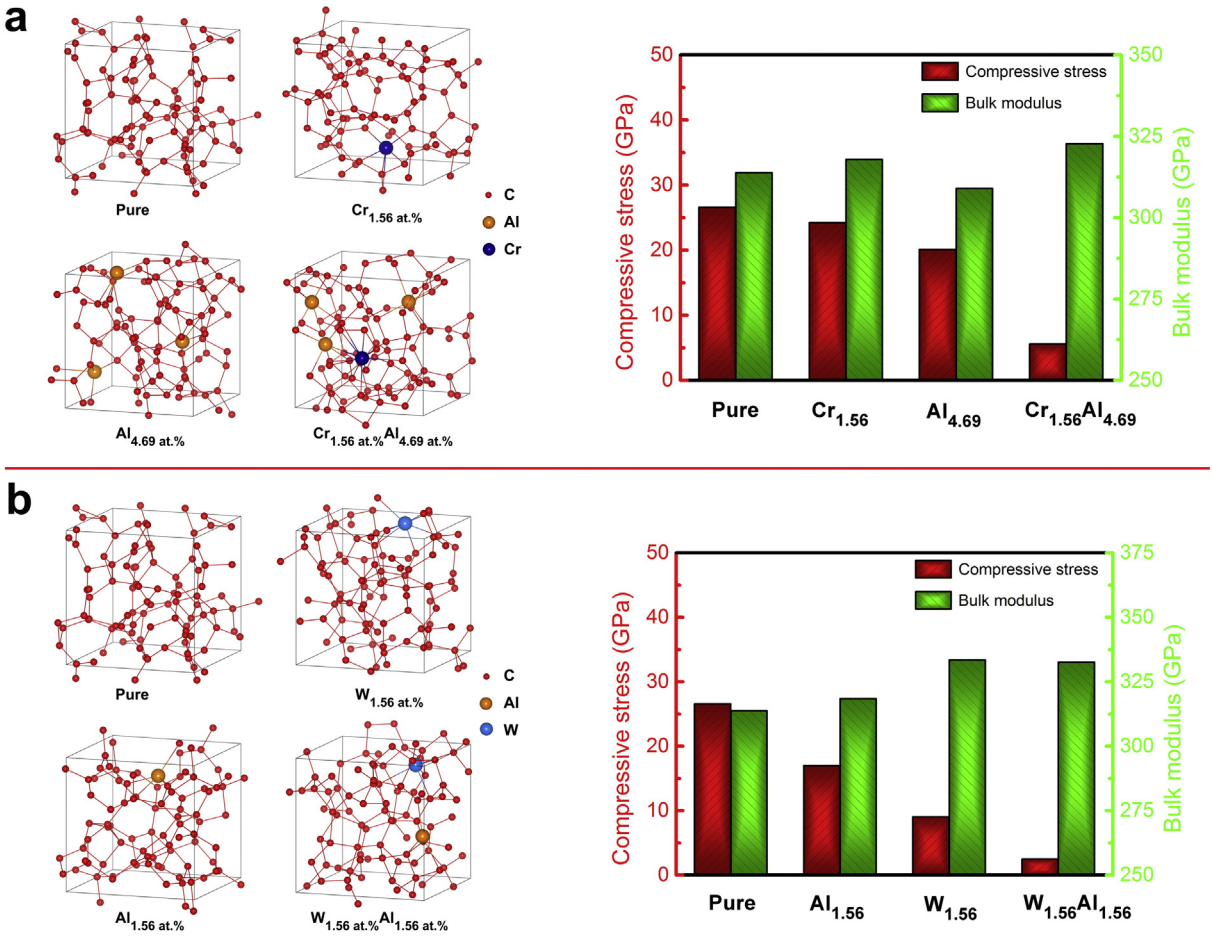

Fig. 8. Atomic structures and properties including the compressive stress and bulk modulus of (a) Cr/Al co-doped and (b) W/Al co-doped a-C films. Pure and Cr/Al or W/Al mono-doped cases are also considered. The subscript in each figure is the concentration of each doped metal atoms.

of atomic bond structure can occur without the significant increase of the strain energy due to the formed weak bond characteristics. Consequently, the drastic relaxation of distorted C–C bond lengths and the formation of weak bond characteristics between Ti/Al and C atoms are supposed to be the fundamental reasons why the residual stress is significantly decreased due to the Ti/Al co-doping.

Similar to the Ti/Al co-doped case, the Cr/Al and W/Al mono- and co-doped a-C systems were also evaluated using the same method. Fig. 8 shows the final structures and the calculated properties including the residual compressive stress and bulk modulus. It reveals that all of the films are amorphous (Fig. 8). Compared with the pure and Cr/Al mono-doped cases (Fig. 8a), co-doping Cr/Al into a-C matrix could further decrease the residual compressive stress; when the co-doped Cr and Al contents are 1.56 and 4.69 at.%, respectively, the residual stress reduces to 5.6 from 24.2 of Cr (1.56 at.%) and 20.1 GPa of Al (4.69 at.%) mono-doped cases, while the bulk modulus increases to 322.7 from 317.8 (only Cr 1.56 at.%) and 309 GPa (only Al 4.69 at.%). By contrast with pure a-C film, the co-doping of Cr/Al could decrease the compressive stress by 78.9% with the increase of bulk modulus by 2.9%. The analysis of distorted bond structure and bond characteristics is shown in Fig. 9a. It indicates that when Cr 1.56 at.% and Al 4.69 at.% are doped into a-C film simultaneously, the fraction of distorted bond angles (<109.5°) slightly increases to 44.2% from 40.9% of Cr (1.56 at.%) and 42.7% of Al (4.69 at.%) mono-doped cases, but that of distorted bond lengths (<1.42 Å) drops to 12.4% remarkably from 22.4% of Cr (1.56 at.%) and 16.9% of Al (4.69 at.%) mono-doped cases. Moreover, the electronic structure (Fig. 9a) shows that the co-doped Cr and Al atoms also bond with C atoms in the form of weak covalent and ionic bonds, respectively. So the combination of critical relaxation of the C–C distorted bond lengths and weak bond characteristics caused by Cr/Al co-doping contributes to the obvious reduction of the residual compressive stress.

For the W/Al co-doped a-C film, Fig. 8b shows that compared with the compressive stress of pure a-C, W 1.56 at.%, and Al 1.56 at.% mono-doped cases (corresponding to 26.6, 9.0, and 17 GPa, respectively), it is seriously reduced to 2.5 GPa when the W 1.56 at.% and Al 1.56 at.% are co-doped. Especially, it is observed that the bulk modulus increases to 332.6 from 333.5 (only W 1.56 at.%) and 318.4 GPa (only Al 1.56 at.%). In contrast with pure case, the co-doping of W/Al could lead to the compressive stress decreased by 90.6% following the increase of bulk modulus by 6%. Furthermore, the fractions of distorted bond angles for W (1.56 at.%) or Al (1.56 at.%) mono-doped films are 42.7% and 42.2%, and those of distorted bond lengths are 15.3% and 20.1%, respectively, as shown in Fig. 9b. Although the fraction of distorted bond angles (<109.5°) shows a little increases (44.1%), that of distorted bond lengths (<1.42 Å) declines up to 11.6% drastically. On the other hand, Fig. 9b also shows the similar bond characteristics, weak covalent bond for W-C and ionic bond for Al–C. These factors account for the behavior of the residual stress caused by W/Al co-doping.

4. Conclusions

In this study, ab initio calculations based on DFT were employed to prepare Ti/Al, Cr/Al, or W/Al co-doped a-C films by a two-step process composed of melt-quenching from liquid and geometric optimization. The residual stress and bulk modulus were calculated, and the atomic and electronic bond structure was analyzed to clarify the stress reduction mechanism. Compared with pure and mono-doped a-C films, the co-doping of Ti/Al, Cr/Al, or W/Al could reduce the residual stress remarkably without the expense of mechanical properties; as Ti (1.56 at.%)/Al (1.56 at.%), Cr (1.56 at.%)/Al (4.69 at.%), or W (1.56 at.%)/Al (1.56 at.%) were co-doped, the residual compressive stress reduced to 4.6, 5.6, and 2.5 GPa separately from 26.6 GPa of pure case. The structure analysis revealed that although co-doping Ti/Al, Cr/Al, or W/Al into a-C

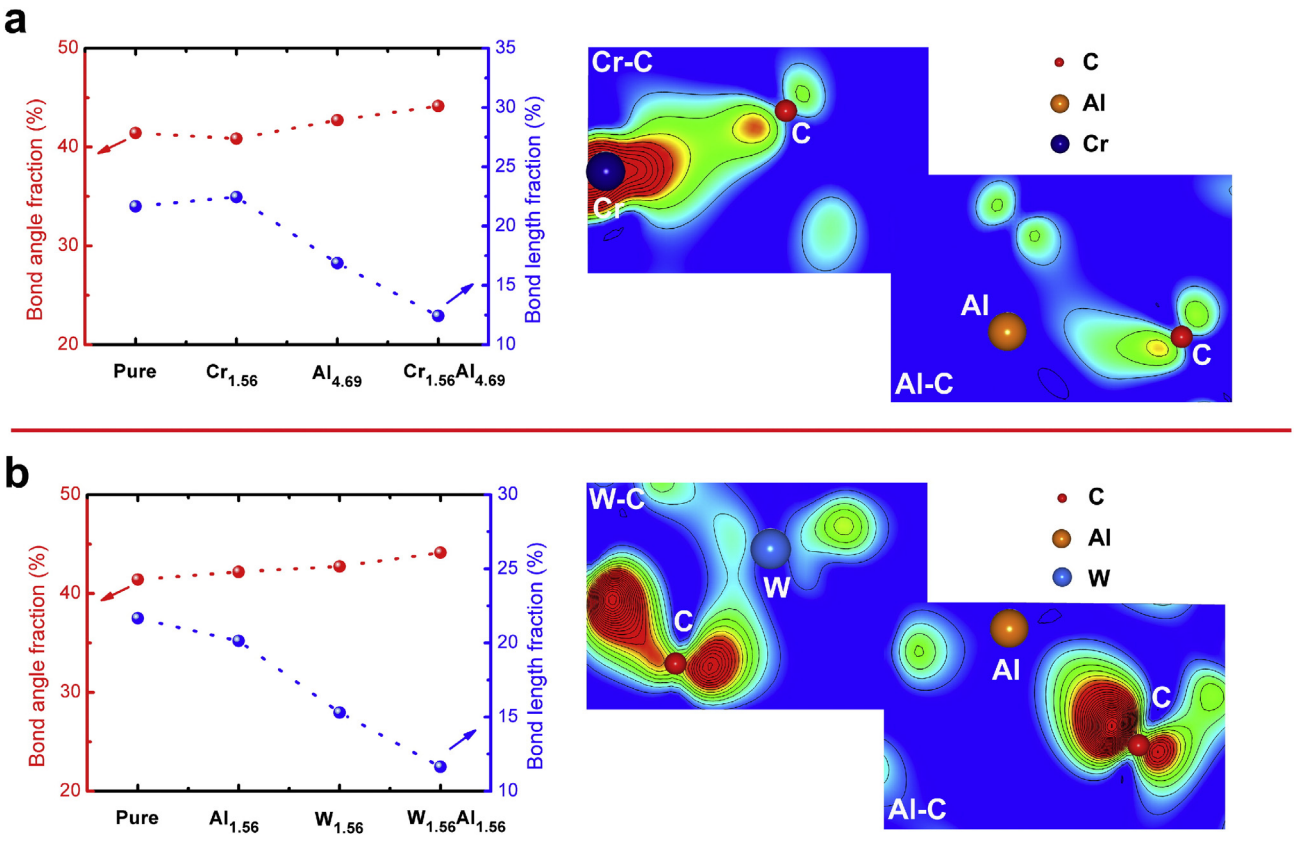

Fig. 9. Fractions of distorted bond angles (<109.5°) and bond lengths (<1.42 Å) and bond characteristics of (a) Cr/Al co-doped and (b) W/Al co-doped a-C films. The subscript in each figure is the concentration of each doped metal atoms.

film causes the slight increase of fractions of the distorted bond angles smaller than 109.5°, the fractions of the distorted bond lengths smaller than 1.42 Å drastically declined to 16.2%, 12.4%, and 11.6%, respectively, from 21.7% of pure a-C film. On the other hand, electronic structure calculation indicated that weak covalent interaction was formed between Ti, Cr or W and C atoms, while the ionic interaction was observed for the Al–C bond. Therefore, the co-doping of Ti/Al, Cr/Al, or W/Al could not only provide the key relaxation of distorted C–C bond lengths, but also play a pivotal site to reduce the increase of strain energy change caused by distortion of bond structure due to the formed weak bonding characteristics, which can resulted in the giant residual stress reduction. The current result provides further insight into the structure and stress reduction mechanism for the previous experimental work, but the more important is that it provides a straightforward possibility by using the synergistic benefits from the binary doped metal feature to fabricate the new nano-composite carbon-based films with high performance for the promising wider applications.

Acknowledgments

This research was supported by the State Key Project of Fundamental Research of China (2013CB632302), National Natural Science Foundation of China (51402319), International Cooperation Foundation of Ningbo Government (2015D10004), and Ningbo Municipal Natural Science Foundation (2014A610001).

References

[1] J. Robertson, Diamond-like amorphous carbon, Mater. Sci. Eng. 37 (2002) 129–281.
[2] L. Wang, R. Zhang, U. Jansson, N. Nedfors, A near-wearless and extremely long lifetime amorphous carbon film under high vacuum, Sci. Rep. 5 (2015), 11119-1–13.
[3] K. Bewilogua, D. Hofmann, History of diamond-like carbon films—from first experiments to worldwide applications, Surf. Coat. Technol. 242 (2014) 214–225.
[4] H.S. Hsu, P.E. Lu, C.W. Chang, S.J. Sun, C.H. Lee, H.C. Su, Y.Y. Chin, H.J. Lin, C.T. Chen, M.J. Huang, Tunable interfacial magnetic-optical properties of Co doped amorphous carbon film induced by charge transfer after acid treatment, Carbon 77 (2014) 398–404.
[5] N. Dwivedi, S. Kumar, J.D. Carey, R.K. Tripathi, H.K. Malik, M.K. Dalai, Influence of silver incorporation on the structural and electrical properties of diamond-like carbon thin films, ACS Appl. Mater. Interfaces 5 (2013) 2725–2732.
[6] J. Wang, J. Pu, G. Zhang, L. Wang, Interface architecture for superthick carbon-based films toward low internal stress and ultrahigh load-bearing capacity, ACS Appl. Mater. Interfaces 5 (2013) 5015–5024.
[7] J. Vetter, 60 years of DLC coatings: historical highlights and technical review of cathodic arc processes to synthesize various DLC types, and their evolution for industrial applications, Surf. Coat. Technol. 257 (2014) 213–240.
[8] J. Huang, L. Wang, B. Liu, S. Wan, Q. Xue, In vitro evaluation of the tribological response of Mo-doped graphite-like carbon film in different biological media, ACS Appl. Mater. Interfaces 7 (2015) 2772–2783.
[9] X. Yu, Y. Qin, C.B. Wang, Y.Q. Yang, X.C. Ma, Effects of nanocrystalline silver incorporation on sliding tribological properties of Ag-containing diamond-like carbon films in multi-ion beam assisted deposition, Vacuum 89 (2013) 82–85.
[10] W. Dai, A. Wang, Q. Wang, Microstructure and mechanical property of diamond-like carbon films with ductile copper incorporation, Surf. Coat. Technol. 272 (2015) 33–38.
[11] Z. Fu, C. Wang, W. Zhang, W. Wang, W. Yue, X. Yu, Z. Peng, S. Lin, M. Dai, Influence of W content on tribological performance of W-doped diamond-like carbon coatings under dry friction and polyalpha olefin lubrication conditions, Mater. Des. 51 (2013) 775–779.
[12] W. Dai, A.Y. Wang, Deposition and properties of Al-containing diamond-like carbon films by a hybrid ion beam sources, J. Alloys Compd. 509 (2011) 4626–4631.
[13] C.S. Lee, K.R. Lee, K.Y. Eun, K.H. Yoon, J.H. Han, Structure and properties of Si incorporated tetrahedral amorphous carbon films prepared by hybrid filtered vacuum arc process, Diam. Relat. Mater. 11 (2002) 198–203.
[14] A.Y. Wang, H.S. Ahn, K.R. Lee, J.P. Ahn, Unusual stress behavior in W-incorporated hydrogenated amorphous carbon films, Appl. Phys. Lett. 86 (2005), 111902-1–3.
[15] N.K. Manninen, F. Ribeiro, A. Escudeiro, T. Polcar, S. Carvalho, A. Cavaleiro, Influence of Ag content on mechanical and tribological behavior of DLC coatings, Surf. Coat. Technol. 232 (2013) 440–446.
[16] V. Singh, J.C. Jiang, E.I. Meletis, Cr-diamondlike carbon nanocomposite films: systhesis, characterization and properties, Thin Solid Films 489 (2005) 150–158.
[17] O. Wilhelmsson, M. Rasander, M. Carlsson, E. Lewin, B. Sanyal, U. Wiklund, O. Eriksson, U. Jansson, Design of nanocomposite low-friction coatings, Adv. Funct. Mater. 17 (2007) 1611–1616.
[18] X. Pang, J. Hao, P. Wang, Y. Xia, W. Liu, Effects of bias voltage on structure and properties of TiAl-doped a-C:H films prepared by magnetron sputtering, Surf. Interface Anal. 43 (2011) 677–682.
[19] X. Pang, L. Shi, P. Wang, Y. Xia, W. Liu, Effects of Al incorporation on the mechanical and tribological properties of Ti-doped a-C:H films deposited by magnetron sputtering, Curr. Appl. Phys. 11 (2011) 771–775.
[20] X. Liu, J. Yang, J. Hao, J. Zheng, Q. Gong, W. Liu, A near-frictionless and extremely elastic hydrogenated amorphous carbon film with self-assembled dual nanostructure, Adv. Mater. 24 (2012) 4614–4617.
[21] G. Kresse, J. Furthmüller, Efficiency of ab initio total energy calculations for metals and semiconductors using plane-wave basis set, Comput. Mater. Sci. 6 (1996) 15–50.
[22] G. Kresse, J. Furthmüller, Efficient iterative schemes for ab initio total-energy calculations using a plane-wave basis set, Phys. Rev. B 54 (1996) 11169–11186.
[23] J.P. Perdew, K. Burke, M. Ernzerhof, Generalized gradient approximation made simple, Phys. Rev. Lett. 77 (1996) 3865–3868.
[24] X. Li, P. Ke, A. Wang, Probing the stress reduction mechanism of diamond-like carbon films by incorporating Ti, Cr, or W carbide-forming metals: ab initio molecular dynamics simulation, J. Phys. Chem. C 119 (2015) 6086–6093.
[25] B. Zheng, W.T. Zheng, K. Zhang, Q.B. Wen, J.Q. Zhu, S.H. Meng, X.D. He, J.C. Han, First-principle study of nitrogen incorporation in amorphous carbon, Carbon 44 (2006) 962–968.
[26] F. Alvarez, C.C. Díaz, R.M. Valladares, A.A. Valladares, Ab initio generation of amorphous carbon structures, Diam. Relat. Mater. 11 (2002) 1015–1018.
[27] M.M.M. Bilek, D.R. McKenzie, D.G. McCulloch, C.M. Goringe, Ab initio simulation of structure in amorphous hydrogenated carbon, Phys. Rev. B 62 (2000) 3071–3077.
[28] D.G. McCulloch, D.R. McKenzie, C.M. Goringe, Ab initio simulations of the structure of amorphous carbon, Phys. Rev. B 61 (2000) 2349–2355.
[29] A. Gambirasio, M. Bernasconi, Ab initio study of boron doping in tetrahedral amorphous carbon, Phys. Rev. B 60 (1999) 12007–12014.
[30] M.J. Gillan, Calculation of the vacancy formation energy in aluminum, J. Phys. Condens. Matter 1 (1989) 689–711.
[31] R. Haerle, G. Galli, A. Baldereschi, Structural models of amorphous carbon surfaces, Appl. Phys. Lett. 75 (1999) 1718–1720.
[32] W. Dai, P. Ke, M.W. Moon, K.R. Lee, A. Wang, Investigation of the microstructure, mechanical properties and tribological behaviors of Ti-containing diamond-like carbon films fabricated by a hybrid ion beam method, Thin Solid Films 520 (2012) 6057–6063.
[33] F. Li, J.S. Lannin, Radial distribution function of amorphous carbon, Phys. Rev. Lett. 65 (1990) 1905–1908.
[34] K.W.R. Gilkes, P.H. Gaskell, J. Robertson, Comparison of neutron scattering data for tetrahedral amorphous carbon with structural models, Phys. Rev. B 51 (1995) 12303–12312.
[35] K.J. Koivusaari, T.T. Rantala, S. Leppävuori, Calculated electronic density of states and structural properties of tetrahedral amorphous carbon, Diam. Relat. Mater. 9 (2000) 736–740.
[36] X. Li, P. Ke, H. Zheng, A. Wang, Structural properties and growth evolution of diamond-like carbon films with different incident energies: a molecular dynamics study, Appl. Surf. Sci. 273 (2013) 670–675.
[37] D.R. McKenzie, D. Muller, B.A. Pailthorpe, Compressive stress induced formation of thin film tetrahedral amorphous carbon, Phys. Rev. Lett. 67 (1991) 773–776.
[38] N.A. Marks, Evidence for subpicosecond thermal spikes in the formation of tetrahedral amorphous carbon, Phys. Rev. B 56 (1997) 2441–2446.